

Meridional circulation and reverse advection in hot thin accretion discs

Pavel Abolmasov^{*}

*Tuorla Observatory, Department of Physics and Astronomy, University of Turku, Väisäläntie 20, FI-21500 Piikkiö, Finland
Sternberg Astronomical Institute, Moscow State University, Universitetsky pr. 13, Moscow 119992, Russia
Kavli Institute for Theoretical Physics, University of California, Santa Barbara, CA 93106, USA*

Accepted —. Received —; in original form —

ABSTRACT

In standard accretion discs, outward angular momentum transfer by viscous forces is compensated by the inward motion of the accreting matter. However, the vertical structure of real accretion discs leads to meridional circulation with comparable amplitudes of poloidal velocities. Using thin-disc approximation, we consider different regimes of disc accretion with different vertical viscosity scalings. We show that, while gas-pressure-dominated discs can easily have a midplane outflow, standard thin radiation-pressure-dominated disc is normally moving inwards at all the heights. However, quasi-spherical scaling for pressure ($p \propto \varpi^{-5/2}$) leads to a midplane outflow for a very broad range of parameters. In particular, this may lead to a reversed, outward heat advection in geometrically thick discs when the temperature decreases rapidly enough with height. While the overall direction of heat advection depends on the unknown details of vertical structure and viscosity mechanisms, existence of the midplane counterflow in quasi-spherical flows is a robust result weakly dependent on the parameters and the assumptions of the model. Future models of thick radiatively inefficient flows should take meridional circulation into account.

Key words: accretion, accretion discs – hydrodynamics – MHD

1 INTRODUCTION

One of the main assumptions of the standard thin disc approach (Shakura & Sunyaev 1973) is locality of energy release: all the heat dissipated inside an annulus is promptly radiated from the surface. This assumption works well as long as (i) the geometrical thickness of the disc is small (that ensures relatively strong vertical gradients of the principal physical quantities) and (ii) energy dissipation time scales are smaller than the time scales of radial motion. Violation of the first assumption makes radiation transport more complex, as the radiation energy density gradient is no more vertical and diffusion coefficient variations with radius also become significant. Violation of the second approximation due to either low emissivity (as in radiatively inefficient advection-dominated flows, see Narayan & Yi 1995a) or high optical depth (as in slim discs, see Abramowicz et al. 1988; Sądowski 2011) means that the radial heat advection is important. Energy dissipated at some radius is then either emitted from some other portion of the disc, or absorbed by the black hole, making the flow radiatively inefficient.

In steady-state accretion flows, as the mechanical energy of the flow is transformed into heat and radiation, the matter should in general move inwards, which makes it logical to assume that advection transports energy inwards with the radial velocity of the flow. There are however indications for non-trivial radial velocity profiles in certain types of accretion discs. In particular, for isothermal, gas-pressure-dominated discs, it was shown already by Urpin (1984) that the radial velocity can easily have the opposite (positive, if negative corresponds to inward motion) sign near the equatorial plane. This finding was confirmed by numerical simulations (Fromang et al. 2011; Stoll & Kley 2016; Philippov & Rafikov 2017) and seems to be a usual feature for thin disc solutions with local, Newtonian-type viscosity, expected in protoplanetary discs around young stars. As it was shown by Philippov & Rafikov (2017), equation (6), equatorial-plane radial velocity is sensitive not to the vertically-integrated viscous stress, as vertically-averaged radial velocity in the standard model, but to the local viscous stress $w_{\varpi\varphi}$ and its dependence on radial (cylindrical) coordinate ϖ . More specifically, if $w_{\varpi\varphi}\varpi^2$ decreases with ϖ , one should expect an equatorial-plane outflow. In discs powered by accretion, this effect can alter the sign of the advection term in energy equation. In contrast

^{*} pavel.abolmasov@gmail.com

with protoplanetary discs, temperature in accretion discs tends to decrease strongly with height, hence it is most likely that the matter bearing most of the heat is moving inwards at a lower-than-average velocity or, perhaps, even moves outwards.

In local Newtonian-type viscosity approach, where the stress is proportional to the strain, one should also take into account the angular velocity dependence on vertical coordinate. Even though for thin discs angular frequency changes only slightly with height, its second vertical derivative is of the same order as the second order radial derivative, and thus may contribute significantly to angular momentum transport. This effect makes the angular momentum transport problem more complicated, but is straightforward to account for in certain assumptions about the vertical structure.

In gas-dominated parts of a standard disc, pressure decreases with radius rapidly enough to suggest a midplane outflow, if viscous stress scales linearly with pressure (the approach we will hereafter call local α -assumption). However, the effects of advection are very small in gas-dominated discs. On the other hand, simple dimensional arguments suggest that, whenever advection is strong and accretion disc becomes thick, the speed of sound scales with virial velocity $c_s \propto \varpi^{-1/2}$, and pressure becomes a very steep function of radius, $p \propto \varpi^{-5/2}$, which is strongly suggestive for existence of a midplane outflow in any type of a thick disc.

It is of course difficult to extrapolate the results obtained in thin-disc approximation to geometrically thick flows. However, it is possible to make estimates for the midplane radial velocity which do not rely much on the assumption of disc thickness.

The goals of this paper are to estimate the vertical rotational structure and two-dimensional angular momentum transport in thin accretion discs where the vertical and radial structure may be decoupled, and to use this approach to estimate the direction of heat advection in different kinds of accretion discs and flows. In Section 2, we formulate the problem and introduce the notation used throughout the paper. Then, in Section 3, we calculate the vertical structure of the angular frequency field. In Section 4 we use different local viscosity models to recover the expected angular momentum transfer and the poloidal velocity field. In Section 5, we show that existence of a midplane outflow in an accretion disc often leads to outward advection of the energy stored as trapped radiation. In Section 6, we discuss the validity of the assumptions used and consider the possible extensions of the model.

2 BASIC ASSUMPTIONS AND NOTATION

We will use cylindrical coordinates z and ϖ , where z is the height above the equatorial plane, and ϖ is the distance towards the axis. We assume stationarity and axisymmetry. Poloidal velocity components are always negligible in comparison with the azimuthal component $v_\varphi = \varpi\Omega$. We assume that above the finite height of $z = H$, density and pressure in the accretion disc become zero. We will also neglect all the terms of the order $(H/\varpi)^2$ and higher in dynamical equations, and assume that, for every physical quantity $f = f(\varpi, z)$, it is possible to separate the variables as $f = f_\varpi(\varpi)f_z(z/H(\varpi))$. Besides, all the radial dependences are assumed smooth and approximated by power laws using notation $f_\varpi \propto \varpi^{-\Gamma_f}$. Rotation velocity Ω is assumed close to Keplerian $\Omega_K = \sqrt{GM}\varpi^{-3/2}$ with accuracy $\sim (H/\varpi)^2$. As the angular momentum transfer equation for Newtonian-type viscosity contains second vertical derivatives of angular frequency $\partial^2\Omega/\partial z^2 \sim \Omega/H^2$, vertical variations of rotation velocity, though negligibly small by themselves, produce a significant contribution to the angular momentum transport equation.

The set of assumptions we use is supposed to reproduce the main properties of the standard α -disc after vertical integration. Strong deviations from the standard model may arise in the models where the viscous stress does not zero at the surface of the disc that implies angular momentum exchange with some ambient medium, such as wind or corona. We will assume that the viscous stress zeroes at the surface.

Dynamical equations we use below are derived from the stationary momentum (Navier-Stokes) equation

$$\rho(\mathbf{v}\nabla)\mathbf{v} = -\nabla p - \rho\nabla\Phi - \nabla\mathbf{w}, \quad (1)$$

where \mathbf{w} is the second-rank viscous stress tensor, components of which are assumed small with respect to pressure. We also suggest that, as poloidal velocity is everywhere smaller than azimuthal, only $w_{r\varphi} = w_{\varphi r}$ and $w_{z\varphi} = w_{\varphi z}$ should be taken into account. Together, these two assumptions imply that only the φ component of equation (1) is affected by viscosity.

Standard disc model uses all these assumptions, but only for vertically-integrated quantities, as the viscosity processes operating in real accretion discs are presumably determined by the characteristic spatial scales of accretion disc thickness. When viscosity is determined by microphysics (ionic or radiative viscosity), kinetic theory (Pitaevskii & Lifshitz 2012) predicts Newtonian-viscosity stress-strain relation (expressed in general Cartesian coordinates i, j , and k) of the form

$$w_{ik} = \left(\frac{\partial v_k}{\partial x_i} + \frac{\partial v_i}{\partial x_k} - \frac{2}{3}\delta_{ik} \frac{\partial v_j}{\partial x_j} \right) \nu \rho \simeq \left(\frac{\partial v_k}{\partial x_i} + \frac{\partial v_i}{\partial x_k} \right) \nu \rho, \quad (2)$$

where ν is viscosity coefficient determined by the characteristic spatial l_t and velocity v_t scales of the transfer process. In the case of turbulent viscosity, l_t is characteristic mixing length and v_t is characteristic turbulent viscosity. If magnetic fields dominate momentum transfer, these quantities may be understood as characteristic magnetic loop size and Alfvén velocity. For meso-scale processes with $l_t \sim H$, the stress-strain scaling should be more complex than in Newtonian approximation and may involve finite differences or spatially-averaged partial derivatives instead, but the direction of angular momentum transport should remain approximately the same, while the amplitude of the stress may vary. Thus equation (2) should still work well unless the transfer processes become anisotropic (such as anisotropic turbulent velocity field considered by Wasiutynski 1946). In the latter case, ν is no more scalar, and the direction of viscous angular momentum transfer can differ

from the direction of velocity gradient. This results in additional terms in viscous stress (see, for instance, [Taylor 1973](#) and [Tassoul 2000](#) chapter 8), that may change completely the angular momentum transfer in accretion discs if anisotropy is strong, as in convection-dominated flows ([Quataert & Gruzinov 2000](#); [Igumenshchev 2002](#)). We will not consider the effects of anisotropic momentum transfer in this paper, except a brief discussion in Section 6.1.

For our case, the velocity field may be approximated as a differential rotation field, and

$$\frac{w_{ik}}{\varpi\nu\rho} = (\mathbf{e}_i^\varphi \mathbf{e}_k^r + \mathbf{e}_i^r \mathbf{e}_k^\varphi) \frac{\partial\Omega}{\partial\varpi} + (\mathbf{e}_i^\varphi \mathbf{e}_k^z + \mathbf{e}_i^z \mathbf{e}_k^\varphi) \frac{\partial\Omega}{\partial z}, \quad (3)$$

where expression \mathbf{e}_i^b , for $b = \varpi, z$, or φ , is the i -th component of the corresponding (radial, vertical, or azimuthal) unit coordinate vector of the cylindrical coordinate frame. The relevant, azimuthal, component of the stress tensor gradient then becomes

$$\mathbf{e}_i^\varphi \nabla_k w_{ik} = \frac{1}{\varpi^2} \frac{\partial}{\partial\varpi} \left(\nu\rho\varpi^3 \frac{\partial\Omega}{\partial\varpi} \right) + \varpi \frac{\partial}{\partial z} \left(\nu\rho \frac{\partial\Omega}{\partial z} \right). \quad (4)$$

This expression is quite general, and the local α -viscosity scaling may be reproduced by substituting $\nu\rho = \alpha p/|\nabla\Omega| \propto \varpi p/\Omega$.

The angular momentum transfer equation is obtained as the azimuthal component of (1)

$$\frac{1}{\varpi} \rho v_\varpi \frac{\partial}{\partial\varpi} (\Omega\varpi^2) = \mathbf{e}_i^\varphi \nabla_k w_{ik}, \quad (5)$$

where the right-hand side will be assumed to be given by (4). In the left-hand side, we neglected the term proportional to v_z , as it is by a factor $\sim \left(\frac{H}{\varpi}\right)^2$ smaller than the radial term.

The other two independent components of the momentum equation will be used to solve for the vertical profiles of pressure and angular frequency. As poloidal velocity components are small, and vertical gradients prevail over radial, vertical component of momentum equation is simply hydrostatic equilibrium condition

$$\frac{\partial p}{\partial z} = -\Omega_K^2 z \rho. \quad (6)$$

As the last of the three independent dynamical equations, it is convenient to use azimuthal component of the curl of equation (1). Neglecting poloidal velocity components, it can be written as (see also [Tassoul 2000](#), equation 27 in chapter 4)

$$\varpi \frac{\partial}{\partial z} (\Omega^2) = \frac{\partial}{\partial z} \left(\frac{1}{\rho} \right) \frac{\partial p}{\partial\varpi} - \frac{\partial}{\partial\varpi} \left(\frac{1}{\rho} \right) \frac{\partial p}{\partial z}. \quad (7)$$

Using equations (6) and (7) allows to calculate the vertical profiles of pressure and angular frequency given the vertical density profile. To recover ρ as a function of z , an additional constraint is needed, that could be effective equation of state or energy equation. Both approaches will be considered in Section 3. Note that existence of a global equation of state $p = p(\rho)$ makes angular frequency constant with height.

3 ROTATION PROFILE

3.1 Analytical approximation

It is convenient to parameterize the vertical density profile as

$$\rho = \rho_c(\varpi) (1 - \xi^2)^a, \quad (8)$$

where $\xi = z/H$, and a is a free parameter. Hydrostatic equation (6) is then easy to integrate obtaining the vertical pressure profile

$$p = p_c(\varpi) (1 - \xi^2)^{a+1}, \quad (9)$$

where

$$p_c = \frac{\Omega_K^2 H^2}{2(a+1)} \rho_c. \quad (10)$$

In the barotropic case, our ansatz corresponds to a polytrope, and a is the polytropic index, $p = \rho^{1+1/a}$. In other cases it can be viewed as an effective polytropic index. In particular, isentropic radiation-pressure-supported disc with $p \propto \rho^{4/3}$ is expected to have $a = 3$. As we will see below, $a = 3$ is a good approximation even for gas-dominated solutions. On the other hand, more sophisticated models of vertical structure ([Ketsaris & Shakura 1998](#); [Shakura et al. 1978](#)) predict $a \simeq 3$ for gas-dominated discs and $a \simeq 1$ for radiation-pressure-dominated discs with convection. Hence, different values of a should be considered.

In such a parameterization, equation (7) takes the form

$$\frac{\partial\Omega}{\partial z} = \frac{a\Gamma_p - (a+1)\Gamma_\rho}{2(a+1)} \frac{z}{\varpi^2} \Omega. \quad (11)$$

Quantities Γ_p and Γ_ρ are logarithmic partial derivatives of central pressure and density, respectively, with respect to ϖ . For the second derivative, neglecting the higher-order terms in z/ϖ ,

$$\frac{\partial^2\Omega}{\partial z^2} \simeq \frac{a\Gamma_p - (a+1)\Gamma_\rho}{2(a+1)} \frac{1}{\varpi^2} \Omega, \quad (12)$$

constant with height as long as the effective polytrope index a is constant. Integration of (11) yields the following, Gaussian angular velocity profile

$$\Omega = \Omega_c e^{\frac{a\Gamma_p - (a+1)\Gamma_\rho}{4(a+1)} \frac{z^2}{\varpi^2}}, \quad (13)$$

where Ω_c is the midplane rotational frequency, equal to Keplerian with an accuracy $\sim (H/\varpi)^2$. Evidently, the sign of $a\Gamma_p - (a+1)\Gamma_\rho$ defines the shape of the isostrophes (surfaces of constant Ω) in the disc near the equatorial plane. Generally, the sign of this combination is negative, hence the isostrophes are convex.

Important special case not covered by the parameterization used here but easily derivable as the limit $a \rightarrow \infty$ is isothermal disc. Density profile has Gaussian shape in this case, hence there is no surface where density approaches zero. Angular frequency derivative becomes

$$\left. \frac{\partial \Omega}{\partial z} \right|_{\text{isothermal}} = (\Gamma_p - \Gamma_\rho) \frac{z}{\varpi^2} \Omega. \quad (14)$$

If pressure decreases with the radial coordinate more rapidly than density, isostrophes are convex, and vertical shear transports angular momentum upwards.

3.2 Numerical solution

It is possible to use a more physical approach by replacing the effective polytrope with assumptions about heat release, radiative transfer and opacity. Vertical structure of thin accretion discs was calculated in a number of papers like Ketsaris & Shakura (1998); Shakura et al. (1978), but here we also track the vertical profile of angular velocity $\Omega(z)$. To check the validity of the effective-polytrope approach for predicting rotational structure and angular momentum transport, we considered the particular case of viscous stress independent of height. This is a reasonable assumption if effective viscosity is provided by magnetic fields (see below Section 4). Details of the vertical structure model are given in Appendix A. Dimensionless mass accretion rate is $\dot{m} = 1$. We normalize the mass accretion rate as $\dot{m} = \frac{\dot{M}c^2}{L_{\text{Edd}}} = \frac{\dot{M}\kappa_{\text{T}}c}{4\pi GM}$, where $\kappa_{\text{T}} \simeq 0.34 \text{ cm}^2 \text{ g}^{-1}$ is Thomson electron scattering opacity. Same definitions are used in Appendix A.

In Fig. 1, we show the sample vertical structure of an accretion disc at different radii, corresponding to different cases of standard disc accretion, particularly to electron-scattering, radiation- and gas-pressure-dominated zones A and B. To calculate Ω , we integrated equation (7) together with the vertical structure equations, assuming power-law dependences on radius for all the midplane quantities. If the vertical structure is described by universal functions of z/H , the variation of disc thickness H with radius does not affect equation (7) as the terms containing $dH/d\varpi$ cancel out:

$$\frac{\partial \ln \Omega}{\partial \xi} = \frac{1}{2\varpi^2 \Omega^2} \frac{p}{\rho} \left(-\Gamma_p \frac{\partial \ln \rho}{\partial \xi} + \frac{\partial \ln \rho}{\partial \xi} \frac{\partial \ln p}{\partial \xi} \Gamma_H + \Gamma_\rho \frac{\partial \ln p}{\partial \xi} - \frac{\partial \ln \rho}{\partial \xi} \frac{\partial \ln p}{\partial \xi} \Gamma_H \right) = \frac{1}{2\varpi^2 \Omega^2} \frac{p}{\rho} \left(\Gamma_\rho \frac{\partial \ln p}{\partial \xi} - \Gamma_p \frac{\partial \ln \rho}{\partial \xi} \right). \quad (15)$$

As it can be seen in Fig. 1, effective polytrope with $a = 3$ is a reasonable estimate for the disc solution with $\nu\rho = \text{const}$ and, probably, for real discs whenever vertical convection does not play important role.

4 ANGULAR MOMENTUM TRANSPORT

Angular momentum transport is governed by two terms, advective and viscous (the left- and right-hand sides of equation 5), that should exactly cancel in stationary case, as angular momentum is a conserved quantity. This allows to estimate the radial velocity as a function of height using equation (5). For a thin disc, it is safe to replace Ω with Ω_{K} (that is of course not true for second derivatives with height).

4.1 Barotropic rotation

This is the case when for some reason the matter of the disc has a global barotropic equation of state. As we will see later, some of the basic properties of barotropic models may be extrapolated to the more general case when Ω variation with height is allowed for.

As it is stated by Poincaré-Wavre's theorem (see Tassoul 2000, section 4.3), angular frequency in a stationary barotropic differentially rotating flow is a function of the cylindrical radial coordinate only. If $\Omega = \Omega(\varpi)$, the second term in the right-hand side of equation (4) becomes zero. For Keplerian rotation, this implies

$$(e_i^\varphi \nabla_k w_{\text{ik}})_{\text{barotropic}} = -\frac{1}{\varpi^2} \frac{\partial}{\partial \varpi} (w_{r\varphi} \varpi^2). \quad (16)$$

As it is easy to see, the sign of the whole expression, and, subsequently, the radial velocity in the midplane is defined by the radial dependence of the local viscous stress: if $w_{\varpi\varphi} \varpi^2$ decreases with radius, there will be a counterflow in the midplane. If rotation is close to barotropic, this quantity is also representative for mean radial velocity. In particular, local-alpha approach predicts

$$v_{\varpi} = -\frac{2\alpha}{\Omega \varpi^2 \rho} \frac{\partial}{\partial \varpi} (p \varpi^2). \quad (17)$$

One of the consequences is that if the variables are separable and equation of state is barotropic (or pseudo-barotropic), the sign of radial velocity does not change with vertical coordinate. The sign of the radial velocity is defined by pressure dependence on ϖ . If $\Gamma_p < -2$, the

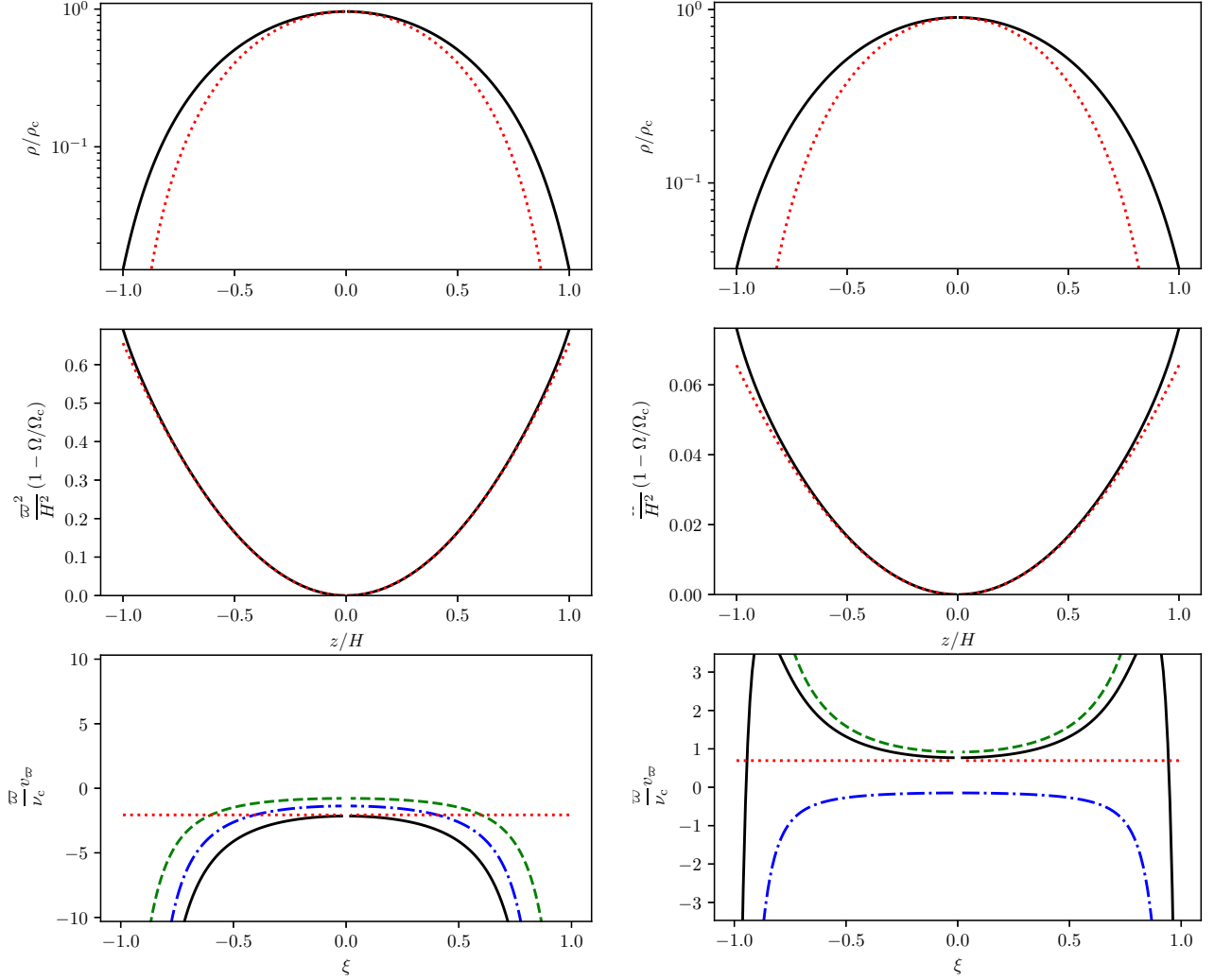


Figure 1. Vertical structure of constant-stress accretion in radiation-pressure- (left panels) and gas-pressure-dominated regimes. Dimensionless mass accretion rate is $\dot{m} = 1$ for both cases, distance from the central object $\varpi = 100$ and $1000 \frac{GM}{c^2}$. Upper, middle and lower panels show density profiles, angular frequency variations, and radial velocities, respectively. Velocities are normalized over characteristic values. Red dotted lines are predictions of the $a = 3$ effective-polytrope model. Green dashed and blue dot-dashed lines in the lower panels correspond to radial and vertical shear contributions to radial velocity (shown in black solid).

sign of v_ϖ is positive, and accretion is impossible. Expression (17) does not rely on the thinness of the disc as long as $z \ll \varpi$, hence it is also valid, for instance, for the midplane of a thick barotropic torus. For a geometrically thick, locally viscous barotropic solution it states that a midplane outflow will be present if the pressure decreases rapidly enough with distance. From dimensional arguments, the radial pressure dependence in thick discs with $H \propto \varpi$ may be shown to depend on radius as $p \propto \varpi^{-5/2}$. Most of the self-similar solutions for thick discs such as the advective disc of Narayan & Yi (1995a) and slim-disc models at large mass accretion rates (Sądowski 2011) reproduce this dependence. Thus, thick barotropic locally-viscous discs should have equatorial outflows.

4.2 General case of isotropic viscosity

A more comprehensive and realistic assumption is that the angular momentum flux is proportional to the local angular velocity gradient, and to use the vertical rotation profile derived in Section 3. Radial dependence of angular frequency is assumed Keplerian $\Omega \propto \varpi^{-3/2}$, as deviations from the Kepler's law are of the order $(H/\varpi)^2$. We will also use the effective polytropic scaling proposed in Section 3.1. Vertical viscosity profile will be described through the free parameter t , $\nu \propto (1 - \xi^2)^t$. For angular momentum flux, we can rewrite equation (4) as

$$e_i^\varphi \nabla_k w_{ik} = \left(-\frac{3}{2} \left(\Gamma_\nu + \Gamma_\rho + \frac{1}{2} + 2\Gamma_H(a+t) \frac{\xi^2}{1-\xi^2} \right) + \frac{a\Gamma_p - (a+1)\Gamma_\rho}{2(a+1)} \left(1 - 2(a+t) \frac{\xi^2}{1-\xi^2} \right) \right) \frac{\nu \rho \Omega}{\varpi}. \quad (18)$$

Here, additional terms proportional to $\xi^2/(1 - \xi^2)$ arise from $\nu\rho$ dependence on height. Consequently, for the radial velocity structure, (5) becomes

$$v_{\varpi} = 2\frac{\nu}{\varpi} \left(A + C\frac{\xi^2}{1 - \xi^2} \right), \quad (19)$$

where

$$A = \frac{a\Gamma_p - (a+1)\Gamma_\rho}{2(a+1)} - \frac{3}{2} \left(\Gamma_\nu + \Gamma_\rho + \frac{1}{2} \right) \quad (20)$$

and

$$C = -(a+t) \left(3\Gamma_H + \frac{a\Gamma_p - (a+1)\Gamma_\rho}{a+1} \right). \quad (21)$$

Coefficient A has the physical meaning of normalized midplane velocity. The second term in (26) does not diverge at the surface of the disc if $t \geq 1$, because the viscosity itself $\nu \propto (1 - \xi^2)^t$. Depending on the quantity of t , velocity may diverge at the surface, but the matter and angular momentum flux are always finite if $a + t \geq 0$. For different model setups, we give the values of A and C in table 1.

The standard-disc scaling for vertically-integrated viscous stress, $\int \rho\nu\varpi \frac{\partial\Omega}{\partial\varpi} dz \propto \int pdz$, may be used to simplify the expressions. In our formalism, it is equivalent to

$$\Gamma_\rho + \Gamma_\nu - \frac{3}{2} = \Gamma_p. \quad (22)$$

For the case of a steady-state disc this may be supplemented with the condition for vertically-integrated viscous stress ignoring the corrections due to the disc inner boundary, $W_{r\varphi} = \frac{1}{2\pi} \dot{M}\Omega \propto R^{-3/2}$. For the thickness determined by the vertical balance, $\Gamma_H = \frac{1}{2}(\Gamma_p - \Gamma_\rho + 3)$, and the standard-disc scaling for the viscous stress, this gives

$$\Gamma_\rho^{\text{stationary}} = 3\Gamma_p + 6, \quad (23)$$

$$\Gamma_\nu^{\text{stationary}} = -2\Gamma_p - \frac{9}{2}, \quad (24)$$

and thus

$$A^{\text{stationary}} = \frac{a}{2(a+1)}\Gamma_p - 3(\Gamma_p + 2). \quad (25)$$

4.3 Condition for an outflow

It is straightforward to check that the expression for the midplane velocity,

$$v_{\varpi}(z=0) = 2A\nu/\varpi, \quad (26)$$

coincides with expression (6) from Philippov & Rafikov (2017). It is interesting to derive a physically motivated criterion for a midplane outflow. Midplane velocity is positive when

$$\Gamma_p \frac{a}{a+1} > 4\Gamma_\rho + 3\Gamma_\nu + \frac{3}{2}. \quad (27)$$

We can safely assume pressure decreasing outwards ($\Gamma_p < 0$) and restrict the possible solutions to positive a , as density is expected to decrease with height. Let us also restrict the possible solutions with the stationary standard disc scaling (25), containing only one free parameter Γ_p . Condition (27) becomes

$$\Gamma_p \frac{a}{a+1} > 6(\Gamma_p + 2). \quad (28)$$

Evidently, an outflow does not exist for any positive value of a if $\Gamma_p > -2$. If $\Gamma_p < -\frac{12}{5} = -2.4$, a midplane outflow exists for all the possible a . Between these values, an outflow exists if

$$a > -\frac{1 + \Gamma_p/2}{1 + \Gamma_p/2.4}. \quad (29)$$

Vertical structure parameter affects the outflow condition only slightly, the main constraints are set upon the radial profiles of certain variables, most importantly – on the viscous stress, or pressure, if the alpha-disc scaling works.

The left-hand side of equation (28) may be also re-written using entropy defined as $s = \ln \frac{p}{\rho^\gamma}$,

$$\frac{\Gamma_p}{\gamma} (1 + s'') > 6(\Gamma_p + 2), \quad (30)$$

where the second entropy derivative is normalized according to Philippov & Rafikov (2017)

$$s'' > \frac{1}{2(a+1)} \frac{\partial^2 s}{\partial \xi^2} = \frac{1}{2(a+1)} \frac{\partial^2}{\partial \xi^2} \ln \left(\frac{p}{\rho^\gamma} \right) \quad (31)$$

Table 1. Vertical structure for parameters relevant for different accretion disc models. “SD” refers to the standard disc model of [Shakura & Sunyaev \(1973\)](#). Averaged velocities are given with accuracy of about one per cent of ν_c/H . Different values of a and t are considered, $t = -a$ reproducing the constant-stress case (we use the $t + a \rightarrow +0$ limit, as described in the text), and $t = 1$ for the local-alpha approximation.

	Γ_ρ	Γ_p	Γ_H	a	t	$a\Gamma_p - (a+1)\Gamma_\rho$	Γ_ν	A	C	$\langle v_\varpi \rangle_\rho H/\nu_c$	$\langle v_\varpi \rangle_p H/\nu_c$
SD zone A	3/2	-3/2	0	3	-3	-21/2	-3/2	-33/16	0	-3.28	-6.77
	3/2	-3/2	0	1	1	-9/2	-3/2	-15/8	0	-1.20	-1.93
SD zone B	-33/20	-51/20	21/20	3	-3	-21/20	3/5	111/160	0	-3.28	2.27
	-33/20	-51/20	21/20	3	1	-21/20	3/5	111/160	-231/20	-1.33	0.84
SD zone C	-15/8	-21/8	9/8	3	-3	-3/8	3/4	57/64	0	-3.28	2.92
	-15/8	-21/8	9/8	3	1	-3/8	3/4	57/64	-105/8	-1.33	-0.77
quasi-spherical	-3/2	-5/2	1	0	0	3/2	1/2	3/2	0	-1.50	3.0
	-3/2	-5/2	1	0	1	3/2	1/2	3/2	-9/2	-1.00	0.60
	-3/2	-5/2	1	3	-3	-3/2	1/2	9/16	0	-3.28	1.85
	-3/2	-5/2	1	3	1	-3/2	1/2	9/16	-21/2	-1.33	-0.88
convective	-1/2	-3/2	1	5/2	-5/2	-2	1/2	-29/28	0	-9.17	-3.22
	-1/2	-3/2	1	5/2	1	-2	1/2	-29/28	-17/2	-3.94	-3.56
	-1/2	-3/2	1	2	-2	-3/2	1/2	-1	0	-8.43	-2.92
	-1/2	-3/2	1	2	1	-3/2	1/2	-1	-15/2	-3.86	-3.44

and the choice of adiabatic index γ is arbitrary as it enters only the definition of s . Solving for the second derivative of entropy yields

$$s'' > 6\gamma - 1 + \frac{12\gamma}{\Gamma_p}, \quad (32)$$

that coincides with the condition (22) from [Philippov & Rafikov \(2017\)](#) in the particular case of stress proportional to pressure. However, the possible values of s'' are limited. The possible effective equations of state are limited by constant density with height, on one hand ($a > 0$, $s'' > -1$), and by the isothermal effective equation of state, on the other ($a < +\infty$, $s'' < \gamma - 1$). Some of these solutions, with $s'' < 0$, are convectively unstable, but still possible because vertical convection is inefficient ([Shakura et al. 1978](#)).

4.4 The role of vertical structure

Of all the possible values of a and t , two cases are the most interesting: the local-alpha case and the constant-stress case. First is important as the simplest generalization of alpha assumption: viscous stress $w_{r\varphi} = \frac{3}{2}\nu\rho\Omega$ is assumed proportional to local pressure that is equivalent to $\Gamma_\nu + \Gamma_\rho - 3/2 = \Gamma_p$ (that reproduces radial behaviour, see above equation 22) and $t = 1$ (vertical profile). The radial scaling for Γ_ν should be also applicable in a more general case, wherever the standard-disc assumption for vertically-integrated quantities $W_{r\varphi} \propto \Pi$ holds.

The other possibility, vertically constant viscous stress, is reproduced by assuming $a + t = 0$ (as the stress is $\sim \nu\rho\Omega$). Physically it is better motivated than local-alpha. Magnetic fields produced by non-linear MRI are expected to be relatively independent of z and easily transported between different z . Large-scale vertical magnetic field should retain its strength to fulfill the flux conservation rule, that suggests constant with height magnetic stresses created by large-scale fields. Vertical structure for a magnetized disc with magnetic field amplitudes independent of vertical coordinate was considered by [Uzdensky \(2013\)](#). Models with $a + t \leq 0$, however, can not reproduce correctly the dynamics of a standard disc, as there is an angular momentum flux through the surface. A compromise we will use in this paper where we restrict ourselves to conservative solutions is to consider the right limit $a + t \rightarrow +0$.

As in the barotropic case, radial velocity in this case does not depend on z ,

$$v_\varpi^{\text{constant stress}} = 2 \left(\frac{a\Gamma_p - (a+1)\Gamma_\rho}{2(a+1)} - \frac{3}{2}(\Gamma_p + 2) \right) \frac{\nu}{\varpi}. \quad (33)$$

Depending on the radial structure of the disc and on the value of a , the value of v_ϖ and its sign may be different. In table 1, we consider several cases important for disc accretion. Along with the standard-disc zones A, B, and C (see [Shakura & Sunyaev 1973](#)) with different assumptions about the vertical structure in density and viscosity, we apply our calculations for the self-similar scalings of a thick quasi-spherical disc and find that, for a broad range of possible parameters, midplane velocity and pressure-weighted radial velocity (the importance of which will be shown in Section 5) are mostly positive. This is in contrast with the classical zone A where the radial velocity is always negative. In gas-pressure-dominated discs, radial velocity sometimes changes sign with vertical coordinate, sometimes not. Except radiation-pressure-dominated thin disc case, midplane velocity is always larger (either positive or smaller by the absolute value) than average.

Apart from standard thin disc approximations, we estimate the properties of the two disc models that in fact assume $H \sim R$. One of these scalings arise if one assumes radial velocity scaling with $\Omega\varpi$ as in advection-dominated solutions (in table 1, we refer to this regime as to quasi-spherical). The other arises from the assumption of strong radial convection. Convection-dominated discs ([Quataert & Gruzinov 2000](#)) tend to have $\Gamma_p \sim -3/2$, hence a midplane outflow is not expected. However, the convection-dominated solution assumes exact

gyrentropic rotation throughout the volume of the disc. Such an equilibrium requires strong convective motions, and neglects other energy transfer processes that can affect the vertical and radial structure of the model. Besides, convective models assume that the velocity field can be easily separated into steady-state smoothly varying part and a fluctuating part providing convective transport. As some simulations of thick discs with convection show (Eggum et al. 1988; Igumenshchev 2002), large convective cells may contribute to velocity field even after averaging in time and radial coordinate. Simulation results also suggest that convection is not efficient enough to lead to gyrentropic rotation.

5 RADIAL HEAT TRANSPORT

5.1 Effective advection velocity

If energy transfer is dominated by diffusive radiation transfer, and adiabatic heating is neglected, energy equation may be written as follows

$$\frac{\partial \varepsilon}{\partial t} + \nabla \mathbf{F} = q, \quad (34)$$

where q is energy dissipation per unit volume, ε is radiation energy density, and $\mathbf{F} = -D\nabla\varepsilon + \mathbf{v}\varepsilon$ is radiation energy flux consisting of a diffusion and an advection parts. In the steady state, $\frac{\partial \varepsilon}{\partial t}$ disappears. To measure the effects of radial advection and diffusion, we should integrate equation (34) over z taking into account the flux Q_{rad} radiated from the surface

$$\frac{\partial}{\partial \varpi} \left(\int D \frac{\partial \varepsilon}{\partial \varpi} dz - \int \varepsilon v_{\varpi} dz \right) = Q_{\text{rad}} - Q_{\text{tot}}, \quad (35)$$

where $Q_{\text{tot}} = \int q dz$. This expression estimates the difference between the fluxes generated inside the accretion disc and radiated from its surface. First term in the left-hand side is suppressed when $\tau \gg 1$, but the second, advective, is potentially important inside the disc. The advective term may be written as $Q_{\text{adv}} = \varepsilon \langle v_{\varpi} \rangle_{\varepsilon}$, where the velocity is averaged with the weights proportional to the energy density

$$\langle v_{\varpi} \rangle_{\varepsilon} = \frac{\int \varepsilon v_{\varpi} dz}{\int \varepsilon dz}. \quad (36)$$

Evidently, averaging with ε (or radiation pressure $p_{\text{rad}} = \varepsilon/3$) does not in general produce the same result as averaging over ρ . As we should reproduce the standard disc equations after integrating the dynamical equations over z ,

$$\langle v_{\varpi} \rangle_{\rho} = \frac{\int \rho v_{\varpi} dz}{\int \rho dz} \quad (37)$$

should be always negative, at least when $a + t > 0$ and there is no stress at the disc surface.

These suggestions are confirmed by direct integration in effective-polytropic approximation. For the velocity expressed by equation (26),

$$\frac{\dot{M}}{2\pi\varpi} = \Sigma \langle v_{\varpi} \rangle_{\rho} = \int \rho v_{\varpi} dz = \frac{2}{\varpi} \int \rho \nu \left(A + C \frac{\xi^2}{1 - \xi^2} \right) dz = \frac{2}{\varpi} \rho_c \nu_c H \left((A - C) G(a + t) + CG(a + t - 1) \right), \quad (38)$$

where

$$G(n) = \int_{-1}^1 (1 - \xi^2)^n d\xi = \frac{\sqrt{\pi} \Gamma(n + 1)}{\Gamma(n + 3/2)}. \quad (39)$$

Substituting A from (20) and C from (21),

$$\Sigma \langle v_{\varpi} \rangle_{\rho} = -\frac{3}{\varpi} \rho_c \nu_c G(a + t) \left(\Gamma_{\nu} + \Gamma_{\rho} + \Gamma_{\text{H}} + \frac{1}{2} \right). \quad (40)$$

The last bracket is proportional to $\frac{\partial}{\partial \varpi} (\nu \rho H \Omega \varpi^2) \propto \frac{\partial}{\partial \varpi} (W_{r\varphi} \varpi^2)$ as it should be in standard theory, and thus does not change sign in a stationary case.

The case of constant viscous stress should be treated separately. Equation (40) can not be reproduced by simply setting $t = -a$, because in this case angular momentum transfer is not conservative. However, it is possible to consider the above set of formulae in the limit $a + t \rightarrow +0$ which produces a different result. Indeed, it is easy to show that

$$\lim_{n \rightarrow +0} n G(n - 1) = 1, \quad (41)$$

hence, for the constant-stress case, equation (26) becomes

$$\langle v_{\varpi} \rangle_{\rho, \text{ constant stress}} = \frac{2}{\varpi} \rho \nu \left(A + \frac{C}{2} \right), \quad (42)$$

that is easily reduced to equation (40) if the values of A and C are substituted using equations (20) and (21). In this limit, the velocity field becomes unphysical: velocity is constant and, generally, different from the mean velocity value. In particular, radial velocity may be positive in every internal point, while the mass transfer is dominated by the infinitely thin surface layer moving inwards. It should be noted that, if in real accretion discs viscous stresses are constant with height, there should be a non-negligible surface stress and thus angular momentum transfer to wind or corona. In our formalism this corresponds to direct substitution of $t = -a$ to equation (18) before integration instead of approaching the limit as it was made above. In this case, $v_{\varpi} = \frac{2A}{\varpi} \frac{\rho \nu}{\Sigma}$. If $A < 0$, this is easily interpreted as angular momentum loss from

the disc surface, while the case of $A \geq 0$ does not have any evident physical meaning as there should not be any angular momentum source at the surface of the disc.

For radiation-pressure-dominated regime, we can replace radiation energy density with pressure and calculate $\langle v \rangle_\varepsilon$ as

$$\begin{aligned} \langle v_\varpi \rangle_\varepsilon &= \frac{\int p v_\varpi dz}{\int p dz} = \frac{\nu_c}{HG(a+1)} ((A-C)G(a+t+1) + CG(a+t)) \\ &= \frac{1}{a+t+\frac{3}{2}} \frac{\nu_c G(a+t)}{HG(a+1)} \left(-\frac{3}{2}(a+t+1) \left(\Gamma_\nu + \Gamma_\rho + \frac{a+t}{a+t+1} \Gamma_H + \frac{1}{2} \right) + \frac{a\Gamma_p - (a+1)\Gamma_\rho}{2(a+1)} \right). \end{aligned} \quad (43)$$

For the particular case of “local-alpha” viscosity when local stress $w_{r\varphi} \propto p$, $t = 1$, and the radial gradients conforming to the quasi-spherical case $\Gamma_\rho = -3/2$, $\Gamma_H = 1$, $\Gamma_p = -5/2$, $\Gamma_\nu = 1/2$:

$$\langle v \rangle_\varepsilon, \text{ quasi-spherical, local-alpha} = -\frac{3}{2} \frac{a^2 - \frac{5}{3}a - 1}{(2a+5)(a+1)} \frac{\nu_c}{H}, \quad (44)$$

that changes sign at $a = (\sqrt{61} - 5)/6 \simeq 0.47$, the stiffer effective polytrope corresponding to positive weighed velocity. Hence, pure “local-alpha” condition easily reproduces inward net advection, always but for exotic, very stiff vertical structure. However, in the more realistic assumption of vertically-constant viscous stress ($t = -a$),

$$\langle v \rangle_\varepsilon, \text{ quasi-spherical, constant stress} = \frac{1}{3} \frac{a+6}{(a+1)G(a+1)} \frac{\nu_c}{H}, \quad (45)$$

that is always positive for positive a .

In Fig. 1, we show not only the density profiles, but also angular velocities and radial velocities calculated using equations (A19) and (A20), respectively. Effective polytropic approximation with $a = 3$ accurately predicts the profile of Ω , as well as the midplane value of v_ϖ , though the velocities at larger heights may deviate strongly due to differences in density profile.

The estimates made above should also be valid for optically thin, radiatively inefficient discs, if thermal conduction is ignored. Thermal conduction will level out temperature gradients, and the likely vertical structure will have $a \gg 1$ (with the case $a \rightarrow \infty$ corresponding to constant temperature). Large a in a quasi-spherical disc means negative or positive $\langle v \rangle_\varepsilon$, depending on the energy release dependence on height. In all the cases, pressure-averaged radial velocity is larger than density-averaged.

5.2 Observational implications

Consequences of non-trivial vertical structure may be well understood in the standard approach to advective discs used, for instance, in Lipunova (1999). The difference between the radiation flux generated inside the disc and that radiated from its surface is expressed through entropy gradient as

$$Q_{\text{adv}} = \int v_\varpi \rho T \frac{\partial s}{\partial r} dz, \quad (46)$$

or, for radiation-pressure-dominated medium,

$$Q_{\text{adv}} = \int v_\varpi \rho \left(\frac{\partial}{\partial r} \left(\frac{\varepsilon}{\rho} \right) + \frac{1}{3} \varepsilon \frac{\partial}{\partial r} \left(\frac{1}{\rho} \right) \right) dz. \quad (47)$$

If the variables are separable, the result is

$$Q_{\text{adv}} = G(a+1) \langle v_\varpi \rangle_\varepsilon \Sigma \left(\frac{\partial}{\partial \varpi} \left(\frac{3\Pi}{\Sigma} \right) + \Pi \frac{\partial}{\partial \varpi} \left(\frac{1}{\Sigma} \right) + \frac{\Pi}{\Sigma} \frac{\partial \ln H}{\partial \varpi} \right). \quad (48)$$

Standard way to use this expression is to replace the mean radial velocity with the density-averaged value (that also absorbs surface density). We can estimate the effects of vertical structure by introducing a discrepancy factor

$$\beta = \frac{\langle v_\varpi \rangle_\varepsilon}{\langle v_\varpi \rangle_\rho}, \quad (49)$$

and assuming power-law dependences on radius for Π and Σ . Thus,

$$Q_{\text{adv}} = -G(a+1)\beta(3\Gamma_\Pi - 4\Gamma_\Sigma + \Gamma_H) \frac{\dot{M}}{4\pi\varpi} \frac{\Pi}{\varpi\Sigma}. \quad (50)$$

The simplest observational manifestation arises from energy balance, $Q_{\text{tot}} = Q_{\text{adv}} + Q_{\text{rad}}$. The observed effective temperature distribution will change affected by radial heat transport as

$$\sigma_B T_{\text{eff}}^4 \simeq \frac{3}{8\pi} \frac{GMM}{\varpi^3} \left(1 - \frac{16}{15} \beta \frac{\varpi}{GM} \frac{\Pi}{\Sigma} \right). \quad (51)$$

This is a rough estimate based on the supposedly power-law radial dependences of all the quantities (we assumed $a = 1$, $\Gamma_\Sigma = -1/2$, $\Gamma_\Pi = -3/2$). It does however show clearly that the corrections that advection introduces in the temperature profile of the disc depend on the ratio of average velocities, and change sign when $\langle v_\varpi \rangle_\varepsilon$ becomes directed outwards. The bracket in expression (51) also estimates the overall change in accretion efficiency.

Change in efficiency is essential for geometrically-thick, advection-dominated flows that should generally conform to the quasi-spherical

scalings discussed above. Such flows are expected to form when cooling is not efficient enough and large part of the released heat is stored inside the disc. Sound speed is limited only by the virial velocity, that implies $H/\varpi \sim 1$, and also suggests virial scaling for other velocity components, and hence $\Gamma_p = -3/2$ and $\Gamma_\rho = -5/2$. As temperatures and radial velocities are high, advection is very important for any type of quasi-spherical solutions. Such flows are expected to appear in two cases: very high and very low mass accretion rates. High mass accretion rate leads to a high luminosity and optical depth, and the photon diffusion time becomes comparable to the viscous timescale. This is the case of slim discs (Abramowicz et al. 1988; Sądowski 2011) and other solutions proposed for super-Eddington accretion (Poutanen et al. 2007). Advection effects are known to limit the luminosity by storing the heat inside the flow absorbed by the black hole. Reverse advection, however, smoothen this effect by spreading the trapped photons to larger disc radii and thus increasing the total luminosity. Radiative efficiency becomes close to that of a standard disc.

The other case is advection-dominated flows expected to exist at low mass accretion rates, about 10^{-2} of Eddington and lower (Yuan & Narayan 2014). Here, transporting the hot gas outwards can again increase the overall efficiency of the flow as the cooling timescale becomes shorter with respect to the viscous and dynamical times at larger radii (Narayan & Yi 1995b). In both cases we expect the flow efficiency to increase due to lower rate of heat advection. However, any type of a radiatively inefficient quasi-spherical flow also differs from the thin disc in sense of dynamics, that we will discuss later in section 6.2.

6 DISCUSSION

6.1 Anisotropic and non-local viscosity

One principal assumption of this work is that viscosity is of Newtonian type, with the stress proportional to strain with equal proportionality coefficients in different directions. This case may be also described as isotropic viscosity, because isotropic turbulent motions reproduce this scaling, and the fourth-rank viscosity tensor reduces to a scalar. However, there are at least two cases when angular momentum transfer can be anisotropic: anisotropic turbulence (created, for instance, by convection) and large-scale magnetic fields. Small-scale chaotic magnetic fields can also produce anisotropic viscosity if their statistical properties favour certain directions in space.

On one hand, anisotropic turbulence can easily change the direction of angular momentum transfer (as suggested by Wasiutynski 1946; for a very general but purely hydrodynamical consideration, see Tassoul 2000, section 8.5). On the other, chaotic magnetic fields produce viscous stresses proportional to strain components. Following Ogilvie (2003), off-diagonal magnetic stress components may be written in linear approximation as

$$w_{(\varpi,z)\varphi} \propto -\varpi B_{\varpi,z} B_\varphi \frac{\partial \Omega}{\partial (\varpi, z)}. \quad (52)$$

Stress components are thus proportional to the corresponding strains, and all the conclusions about the radial angular momentum transfer hold. However, the vertical term must in general be rescaled with the corresponding field component. Numerical simulations of MHD turbulence in saturated state suggest $B_{\varpi,z} \ll B_\varphi$ in Keplerian shear flows (Parkin & Bicknell 2013). Similarly, turbulent velocity dispersion is expected to be dominated by azimuthal motions (Ogilvie 2003). For an anisotropic turbulent velocity field, $\varpi\varphi$ -stress is proportional to

$$w_{\varpi\varphi} \propto \frac{1}{\varpi} \left\langle v_{\text{turbulent},r}^2 \right\rangle \frac{\partial}{\partial \varpi} (\varpi^2 \Omega) - 2 \left\langle v_{\text{turbulent},\varphi}^2 \right\rangle \Omega. \quad (53)$$

Angular momentum transfer direction for predominantly azimuthal velocity field has thus the same direction as for the isotropic case, but becomes proportional to Ω rather than its derivative.

Angular momentum transfer becomes non-local if the spatial scales of the magnetic loops and mixing lengths for turbulent motions become comparable to or larger than disc thickness. Extremely non-local angular momentum transfer is provided by non-axisymmetric global perturbation modes in the disc. In particular, spiral shock waves were recently shown (Jiang et al. 2017) to play important role in radiation-pressure-dominated accretion discs. By definition, such structures are non-linear, non-axisymmetric and non-stationary. This means that the velocity averaging procedure used in section 5 becomes invalid, as there are local heat flows and non-stationary processes connected non-linearly with the local perturbations. More generally, existence of large-scale structures in the disc favoured by many simulations (Jiang et al. 2014; Sądowski & Narayan 2016a) will lead to additional correction factors for the averaged velocity values, most likely increasing the heat transport outwards when the radial entropy gradient is super-adiabatic. For non-local viscous stresses and large-scale inhomogeneities in the disc, it is still possible to describe the angular momentum transfer in terms of Reynolds stress, but its components should depend on the conditions throughout the disc, not only at the radius considered. The $r\varphi$ component of the Reynolds stress is expected to scale approximately with pressure (Balbus 2003, section 3.3) that means one should expect “local-alpha” to be a reasonable description for the average circulation pattern. However, strong deviations from linearity, stationarity and axisymmetry may alter the results.

In the limiting case of large-scale dynamically important magnetic fields and turbulent motions in thick discs, $w_{\varpi z}$ stress component should be also important. In particular, $w_{\varpi z}$ is likely responsible for the smooth radial velocity profile, very weakly dependent on z , in some of the MHD simulations (Sądowski et al. 2014; Sądowski & Narayan 2016b; Jiang et al. 2014). At the same time, certain simulations of thin ($H/R \sim 0.1$) MHD accretion discs (such as Zhu & Stone 2017) tend to reproduce the vertical profiles of radial velocities. Possibly, some disc thickness effects smooth out the radial velocity profiles.

6.2 Effects of disc thickness

Directly, effects of disc thickness are not expected to affect much the results given in this paper. The equation for angular momentum transfer (equation 4) as well as the vertical derivative of angular frequency estimate (equation 7) are valid in general case. All the results near the equatorial plane hold, though the midplane value of angular frequency may change significantly. In particular, the statement about the midplane outflow does not rely strongly on the assumption about disc thickness as all the neglected terms are proportional to $(z/\varpi)^2$ rather than to $(H/\varpi)^2$.

A potentially important issue is the poloidal velocity field. So far we neglected the vertical motions in the disc. They should be negligible near the midplane, but at $z \sim H$ the impact of v_z is important. Equation (5) becomes

$$\frac{1}{\varpi} \rho v_{\varpi} \frac{\partial}{\partial \varpi} (\Omega \varpi^2) + \varpi \rho v_z \frac{\partial \Omega}{\partial z} = e_i^{\varphi} \nabla_k w_{ik}. \quad (54)$$

For a conservative disc, vertical velocities should follow the changes in disc thickness, approximately as $v_z = \Gamma_H \frac{z}{\varpi} v_{\varpi}$. This makes a correction to the expression for steady-state radial velocity

$$v_{\varpi} = v_{\varpi}^{\text{thin-disc}} \cdot \left(1 + \frac{(a\Gamma_p - (a+1)\Gamma_{\rho})\Gamma_H}{a+1} \left(\frac{z}{\varpi} \right)^2 \right). \quad (55)$$

This correction multiplier is unlikely to alter the overall circulation pattern, especially if $\frac{(a\Gamma_p - (a+1)\Gamma_{\rho})\Gamma_H}{a+1} > 0$, that is true for most of the models considered. We suggest that the effects of ϖz viscosity component, angular momentum exchange with the wind or corona, and non-local angular momentum transfer are more important.

7 CONCLUSIONS

We conclude that, in a thin accretion disc with local, isotropic viscosity and no angular momentum loss from the surface, poloidal velocity field is strongly affected by meridional circulation. The principal quantity is the radial slope of the midplane viscous stress $w_{r\varphi}$. If the stress decreases with radius as $w_{r\varphi} \propto \varpi^{-2}$ or faster, a midplane outflow is possible.

Existence of a midplane outflow in geometrically thick accretion discs should be important for advection effects, especially for very high (super-Eddington) mass accretion rates, when optical depth is large and temperature grows rapidly toward the equatorial plane. In thick discs one should expect the viscous stress to depend on the radial coordinate as $w_{r\varphi} \propto \varpi^{-5/2}$ that evidently should lead to an outflow. Depending on the details of vertical structure, energy dissipation and transfer, advective heat flux may be dominated either by the overall radial velocity directed inwards or by the equatorial counterflow. The effective radial velocity of heat transfer may differ from the density-averaged velocity by a factor of several.

ACKNOWLEDGMENTS

I would like to thank Galina Lipunova, Alexander Philippov, Alexander Tchekhovskoy, Phil Armitage, and Richard Nelson for valuable discussions. Special thanks to Vyacheslav Zhuravlev who has drawn my attention to the issue of meridional circulation. The work was supported by the Academy of Finland grant 268740 and the Russian Scientific Council grant 14-12-00146.

REFERENCES

- Abramowicz M. A., Czerny B., Lasota J. P., Szuszkiewicz E., 1988, *ApJ*, **332**, 646
 Balbus S. A., 2003, *ARA&A*, **41**, 555
 Eggum G. E., Coroniti F. V., Katz J. I., 1988, *ApJ*, **330**, 142
 Fromang S., Lyra W., Masset F., 2011, *A&A*, **534**, A107
 Igumenshchev I. V., 2002, *ApJ*, **577**, L31
 Jiang Y.-F., Stone J. M., Davis S. W., 2014, *ApJ*, **796**, 106
 Jiang Y.-F., Stone J., Davis S. W., 2017, preprint, ([arXiv:1709.02845](https://arxiv.org/abs/1709.02845))
 Ketsaris N. A., Shakura N. I., 1998, *Astronomical and Astrophysical Transactions*, **15**, 193
 Lipunova G. V., 1999, *Astronomy Letters*, **25**, 508
 Narayan R., Yi I., 1995a, *ApJ*, **444**, 231
 Narayan R., Yi I., 1995b, *ApJ*, **452**, 710
 Ogilvie G. I., 2003, *MNRAS*, **340**, 969
 Parkin E. R., Bicknell G. V., 2013, *ApJ*, **763**, 99
 Philippov A. A., Rafikov R. R., 2017, *ApJ*, **837**, 101
 Pitaevskii L., Lifshitz E., 2012, *Physical Kinetics*. No. v. 10, Elsevier Science, <https://books.google.ru/books?id=DTHxPDFV0fQC>
 Poutanen J., Lipunova G., Fabrika S., Butkevich A. G., Abolmasov P., 2007, *MNRAS*, **377**, 1187
 Quataert E., Gruzinov A., 2000, *ApJ*, **539**, 809
 Sądowski A., 2011, ArXiv e-prints: 1108.0396,
 Sądowski A., Narayan R., 2016a, *MNRAS*, **456**, 3929

- Sądowski A., Narayan R., 2016b, *MNRAS*, **456**, 3929
 Sądowski A., Narayan R., Tchekhovskoy A., Abarca D., Zhu Y., McKinney J. C., 2014, preprint, ([arXiv:1407.4421](https://arxiv.org/abs/1407.4421))
 Shakura N. I., Sunyaev R. A., 1973, *A&A*, **24**, 337
 Shakura N. I., Sunyaev R. A., Zilitinkevich S. S., 1978, *A&A*, **62**, 179
 Stoll M. H. R., Kley W., 2016, *A&A*, **594**, A57
 Tassoul J., 2000, *Stellar Rotation*. Cambridge Astrophysics, Cambridge University Press, http://books.google.fi/books?id=yWh0MR_xCg8C
 Tayler R. J., 1973, *MNRAS*, **165**, 39
 Urpin V. A., 1984, *Soviet Ast.*, **28**, 50
 Uzdensky D. A., 2013, *ApJ*, **775**, 103
 Wasiutynski J., 1946, *Astrophysica Norvegica*, **4**, 1
 Yuan F., Narayan R., 2014, *ARA&A*, **52**, 529
 Zhu Z., Stone J. M., 2017, preprint, ([arXiv:1701.04627](https://arxiv.org/abs/1701.04627))

APPENDIX A: VERTICAL STRUCTURE IN CONSTANT-STRESS APPROXIMATION

Here, we will consider the vertical structure for the particular case of constant dissipation with height, $\nu\rho = \text{const}$. Basic equations are vertical hydrostatic equilibrium

$$\frac{dp}{dz} = -\Omega^2 \rho z, \quad (\text{A1})$$

optical depth growth

$$\frac{d\tau}{dz} = -\varkappa\rho, \quad (\text{A2})$$

where \varkappa is (Rosseland) opacity, with contributions from free-free absorption and free electron scattering taken into account. Fick's law for radiation diffusion

$$F = -\frac{c}{\varkappa\rho} \frac{d}{dz} (p_r) \quad (\text{A3})$$

where $p_r = \frac{4\sigma_{\text{SB}}}{3c} T^4$ is radiation pressure, σ_{SB} is Stefan-Boltzmann constant, and dissipation law

$$\frac{dF}{dz} = \nu\rho \left(\left(\frac{\partial\Omega}{\partial\varpi} \right)^2 + \varpi^2 \left(\frac{\partial\Omega}{\partial z} \right)^2 \right) = \nu\rho\Omega^2 \left(\frac{9}{4} + \left(\frac{a\Gamma_p - (a+1)\Gamma_\rho}{2(a+1)} \frac{z}{\varpi} \right)^2 \right) \simeq \frac{9}{4} \nu\rho\Omega^2. \quad (\text{A4})$$

Below we will neglect the $O(z/\varpi)^2$ term. Angular frequency is assumed indistinguishable from Keplerian and constant with height (only deviations in second derivative $\frac{\partial^2\Omega}{\partial z^2}$ are important in our assumptions). Together with constancy of dissipation, it allows to integrate equation (A4) directly as

$$F = \frac{9}{4} \nu\rho\Omega^2 z. \quad (\text{A5})$$

Density may be normalized as follows:

$$\rho = \frac{\Sigma}{H} \tilde{\rho} = \frac{2\tau_0}{\varkappa_T H} \tilde{\rho}, \quad (\text{A6})$$

where $\varkappa_T \simeq 0.34 \text{cm}^2 \text{g}^{-1}$ is Thomson opacity, and $\tau_0 = \varkappa_T \Sigma / 2$ is the total Thomson opacity from the equatorial plane to the infinity along the vertical coordinate. Analogously,

$$p = \frac{2\tau_0 H \Omega^2}{\varkappa_T} \tilde{p}. \quad (\text{A7})$$

The same normalization will be used for radiation pressure. The kinematic viscosity is determined by the largest scales and largest velocities reachable for MHD turbulence, hence $\nu \sim H c_s$. It is convenient to use the same normalization as for pressure for the quantity

$$\nu\rho\Omega = \alpha \frac{2\tau_0 H \Omega^2}{\varkappa_T}, \quad (\text{A8})$$

where α is a free parameter similar in physical meaning to the thin-disc α parameter.

Energy radiated from one side of the disc may be used to link the mass accretion rate with disc thickness as

$$\frac{3}{8\pi} \frac{GM\dot{M}}{R^3} = F(z=H) = \frac{9}{4} \nu\rho\Omega^2 H, \quad (\text{A9})$$

where we neglected the correction multiplier important near the disc's inner edge. Dimensionless mass accretion rate defined as $\dot{m} = \frac{\varkappa_T c \dot{M}}{4\pi GM}$ and midplane sonic velocity c_s (in c units) may be expressed from each other as

$$\dot{m} = 3\alpha\tau_0 c_s^2 r^{3/2}, \quad (\text{A10})$$

where $c_s = \Omega H / c$.

Finally, the system of equations takes the form

$$\frac{d\tilde{p}_r}{d\xi} = -\frac{9}{2}\alpha\tau_0c_s\frac{\varkappa}{\varkappa_T}\tilde{\rho}\xi, \quad (\text{A11})$$

$$\frac{d\tilde{p}}{d\xi} = -\xi\tilde{\rho}, \quad (\text{A12})$$

$$\frac{d\tau}{d\xi} = -2\tau_0\frac{\varkappa}{\varkappa_T}\tilde{\rho}, \quad (\text{A13})$$

where $\tilde{\rho}$ is found as a function of total and radiation pressure as

$$\tilde{\rho} = \frac{mc^2}{k} \left(\frac{2\sigma_{\text{SB}}\varkappa_T GM}{3c^5} \frac{1}{\tau_0 c_s} \right)^{1/4} r^{3/8} c_s^2 \frac{\tilde{p} - \tilde{p}_r}{\tilde{p}_r^{1/4}} \simeq 1.06 \times 10^5 \left(\frac{M}{M_\odot} \right)^{1/4} \tau_0^{-1/4} c_s^{7/4} r^{3/8} \frac{\tilde{p} - \tilde{p}_r}{\tilde{p}_r^{1/4}}. \quad (\text{A14})$$

Here, m is the mean mass of a particle, set to 0.6 of a proton mass that is a good approximation for a fully ionized solar metallicity plasma. Boundary conditions for the pressure may be set at the photosphere. For total pressure, from the hydrostatic equation,

$$p(\tau = 1) = \frac{GMH}{\varkappa R^3}, \quad (\text{A15})$$

that corresponds, for the normalized quantity, to

$$\tilde{p}(\tau = 1) = \frac{1}{2\tau_0} \frac{\varkappa_T}{\varkappa}. \quad (\text{A16})$$

At the same time, radiation pressure is determined by the local gas temperature, equal to effective temperature at $\tau \simeq 2/3$. As most of the disc has very large optical depth, the difference between $\tau = 0, 2/3$, and 1 is insignificant. Therefore, we can set

$$p_r(\tau = 1) = \frac{4\sigma_{\text{SB}}}{3c} T_{\text{eff}}^4, \quad (\text{A17})$$

that corresponds, for the normalized quantity, to

$$\tilde{p}_r(\tau = 1) = 3\alpha c_s. \quad (\text{A18})$$

Thomson optical depth needs to be τ_0 in the equatorial plane, that sets constrain on the only free parameter of the model, τ_0 .

Once the density and pressure are known as functions of vertical coordinate, rotation profile may be expressed using equation (7) and normalizations introduced in this Appendix

$$\frac{\partial \ln \Omega}{\partial \xi} = \frac{H^2}{2\varpi^2} \frac{\tilde{p}}{\tilde{\rho}} \left(\Gamma_\rho \frac{\partial \ln \tilde{p}}{\partial \xi} - \Gamma_p \frac{\partial \ln \tilde{\rho}}{\partial \xi} \right) = \frac{1}{2} c_s^2 \frac{\varpi c^2}{GM} \frac{\tilde{p}}{\tilde{\rho}} \left(\Gamma_\rho \frac{\partial \ln \tilde{p}}{\partial \xi} - \Gamma_p \frac{\partial \ln \tilde{\rho}}{\partial \xi} \right). \quad (\text{A19})$$

Finally, after solving for the vertical structure, radial velocity may be calculated directly using normalized equations (4) and (5)

$$v_\varpi = 2\frac{\nu c}{\varpi} \left(-\frac{3}{2} \left(\Gamma_\nu + \Gamma_\rho + \frac{1}{2} \right) + \frac{\partial^2 \ln \Omega}{\partial \xi^2} \right) = 2\alpha c_s^2 \sqrt{\frac{\varpi c^2}{GM}} \left(-\frac{3}{2} \left(\Gamma_\nu + \Gamma_\rho + \frac{1}{2} \right) + \frac{\partial^2 \ln \Omega}{\partial \xi^2} \right). \quad (\text{A20})$$